Bone Surface Reconstruction Using Localized Freehand Ultrasound Imaging

4 authors, including:

Marc-Emmanuel Bellemare
Aix-Marseille Université
29 PUBLICATIONS **116** CITATIONS

Some of the authors of this publication are also working on these related projects:

Project ANR-MoDyPe View project

Bone Surface Reconstruction Using Localized Freehand Ultrasound Imaging

Lucero Lopez-Perez$^{\alpha}$, Julien Lemaitre$^{\beta}$, Agung Alfiansyah$^{\gamma}$ and Marc-Emmanuel Bellemare$^{\delta}$

Abstract— We propose a bone surface reconstruction method using localized ultrasound imagery. A set of bone contours is first extracted from a series of freehand 2D B-mode localized images, using an automatic segmentation method. This set is then used to reconstruct the bone surface with a tensor product B-splines approximation. Results of the partial surface reconstruction are shown for real bones and for a phantom physical model.

I. INTRODUCTION

Automatic segmentation of osseous structures in image datasets is an essential pre-processing step for several visualization and analysis tasks, in particular for Computer Assisted Diagnosis (CAD) and Surgery (CAS) applications.

Because of its ease of use, non-invasiveness, availability and low cost, ultrasound (US) imagery is of great interest for minimally-invasive exploration of the body, diagnosis, intervention and therapy purposes. However, US images analysis is made difficult by its strong speckle noise, and currently, bone segmentations from US images are obtained using time-consuming manual or semi-automatic algorithms. We propose an automatic method for segmenting the partial bone surface available from a series of US images, for the case of long shaped bones such as the tibia, humerus, clavicle, ulna or radius.

Our bone surface reconstruction method is presented in Sect. II. Sect. III presents some examples and results on real bones and a phantom model of clavicle, and we conclude in Sect. IV.

II. RECONSTRUCTION METHOD

The reconstruction method is made up of four steps:

A. Ultrasound image acquisition.
B. Automated bone segmentation.
C. Point re-sampling.
D. Surface Reconstruction using B-Splines.

A. Ultrasound Image Acquisition

We use a navigated 7.5Mhz US probe[1] to acquire a series of localized 2D B-mode US images of the bone of interest. These images are considered as slices of a 3D image volume.

The acquisition process is straightforward: the operator drags the probe over the patient skin, keeping the bone of interest in the center of the image.

This process has three intrinsics constraints: the bone must be immobilized, the probe must be visible to the navigation system during the acquisition; and the bone must be visible in the acquired images. Also, the slices should be sorted along a straight axis; however, we do not require them to be parallel to each other. For better restults, the probe should be positioned aligned with the plane orthogonal to the bone.

B. Automated Bone Segmentation

Despite the relatively low visual quality and difficult interpretation of US images, they are widely used in CAD, resulting in a growing number of works on US image segmentation. A wide review is presented in [1].

In [2] the authors propose to perform anisotropic diffusion adapted to the speckle noise on the US images coupled with a fast and simple segmentation procedure. Alternatively, one may use a more detailed segmentation method coupled with a fast regularization step or without regularization at all. Works such as [3] use both robust regularization and segmentation procedures. Because of the time constraints usual for CAD applications, we have chosen the second approach.

Ultrasound images are characterized by strong speckle noise, and the difficulty of their segmentation leads to the use of all available prior information.

To automate the segmentation of the bone contours from the series of 2D slices, we adapt the snake model involved in the hip bone segmentation proposed in [4] and [5] to the case of elongated bone partial contours, such as the ulna, humerus, or clavicle. This model was designed to segment the strong-contrast but noisy US images of bones. The bone contour has been characterized by a bright pixel region, with a light bright region above and a dark region below, which corresponds to the acoustic shadow of the bone (see Fig. 1).

The energy that drives the evolution is defined by an internal energy $E_{Internal}$, which controls the curve $v(s)$: $\mathbb{R} \rightarrow \mathbb{R}^2$ regularity:

$$E_{Internal}(v(s)) = w_1|v'(s)|^2 + w_2|v''(s)|^2 \qquad (1)$$

and an external energy $E_{External}$:

$$E_{External}(v(s)) = F_{Balloon}(v(s)) + E_{Regional}$$

where $F_{Balloon}$ is a balloon-force constraint energy:

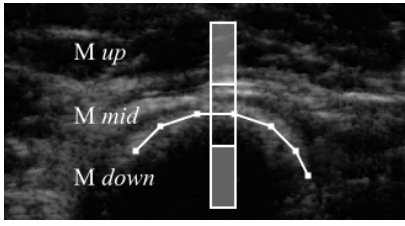$$F_{Balloon}(v(s)) = k_1\vec{N}(v(s)) + k_2\frac{\nabla P}{\|\nabla P\|} \qquad (2)$$

Fig. 1. Intensity regions

a) First snake initialization   b) Regional energy

c) Minimal energy snake   d) Points after post-treatment

Fig. 2. Segmentation Procedure

P is a potential image, $\vec{N}(v(s))$ is the normal to $v(s)$ and $E_{Regional}$ is a regional energy (plotted as the image intensity in Fig. 2b) designed to position the snake in the center of the dark-bright-dark region that characterizes the bone:

$$Dif(v_i) = 2 \times M_{mid} - M_{up} - M_{down}$$

$$E_{Regional} = \left\{ \begin{array}{ll} k & \text{if } Dif(v_i) < 0 \\ Dif(v_i) & \text{otherwise} \end{array} \right. \quad (3)$$

where M_{mid}, M_{up}, M_{down} are the average intensity of the regions depicted on Fig. 1. $F_{Balloon}$ acts as an additional pressure force in the direction normal to the contour in order to avoid the contour converging towards a false local minima.

Our snake is an open active contour with a discrete point curve representation. The minimal energy is estimated with finite elements and finite differences methods (see [4] for details). The iterative energy minimization is stopped when the snake's point displacement becomes less than 3 pixels or if the maximum number of iterations is reached (typically set to 300).

For the hip bone in [4], the snake was initialized with a straight line in the bottom of the image. To shorten the number of iterations needed to segment the bone surface and prevent the snake to converge to local minima, we use the serial acquisition of the section images to initialize the contour. Since the bone is continuous, if we have enough section images of the bone (among 50 and 250 depending on its size), the bone contour should not vary more than 1cm between sections. During the acquisition, the bone contour moves down to the bottom on the image until it reaches the elbow. We initialize the contour of the $(i)th$ image with a horizontal straight line positioned 50 pixels below the minimal height of the $(i-1)th$ image.

In order to keep only snake points which are good candidates to lie on the bone surface, a posterior choice is made by a threshold over its intensity to keep strong intensity pixels only:

$$Intensity(p) > I_{mean} + k_{intensity} \cdot I_{var}$$

where I_{mean} is the mean intensity over the snake points and I_{var} its variance. After the decimation step, only the longest connected segment is kept; we consider two points as connected if their distance is less than 10 pixels (Fig. 2d).

The parameters from 1, 2, and 3 were fixed using the knowldge provided by previous works of the lab team ([5], [4]): $w_1 = 1$, $w_2 = 2.5$, $k_1 = 500$, $k_2 = 0.5$, $k_{intensity} = 0.005$, the number of points in the snake is 100.
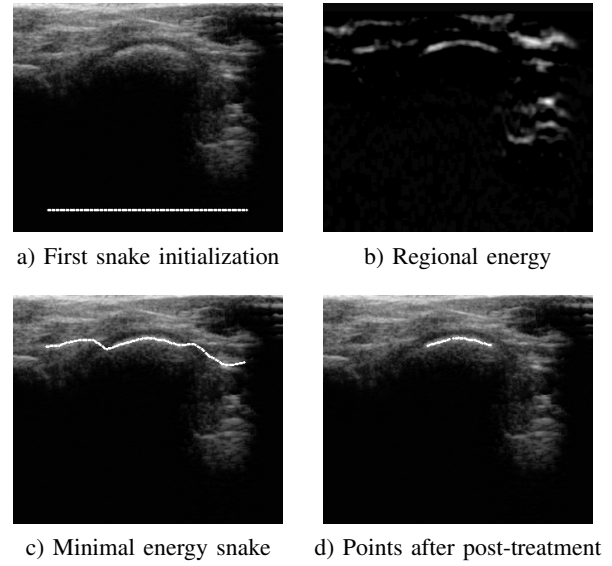
For 5 sets of 50 to 200 images of real forearm bones, we obtain an average 10% of images whose segmented points do not correspond to the bone surface. These false positives correspond to images with important noise on the acoustic shadow under the bone. The phantom examples gave no false positives.

To overcome false results, we performed an anisotropic regularization step before the segmentation procedure. The results were not satisfactory enough to justify the extra-computation time (3 to 5 more seconds per image), instead, we manage the outliers in the surface approximation step.

The summary of the segmentation procedure follows:
1) Initialize the snake for the first slice image by a straight line at half the height of the image.
2) For each slice i:
   a) Compute the minimal energy curve;
   b) Perform the posterior choice of bone points;
   c) Initialize the snake in slice $i+1$ using the current segmentation result.

C. Point Re-sampling

We aim to build a mesh which approximates a partial surface of the bone from the set of planar contour cross-sections obtained from the segmentation procedure previously described. A first approach would consist in building a Delaunay triangulation directly from the segmented points, however the points distribution in the space is rather inhomogeneous: the x and y coordinates are about 1 mm close, but the z coordinates are separated from 5 to 20 mm. Small segmentation errors would result in bad surface topology. Instead, we use prior knowledge of the cylinder-like local topology of the bones of interest to obtain a convenient re-sampled grid of points that we can use later to fit a B-Spline surface.

A large amount of works addresses the problem of mesh reconstruction from a set of parallel planar cross-sections for

general topology surfaces. Among such studies are found [6], [7], and [8] in particular, where the authors propose a vessel surface extraction method using skeletons and pseudo-cylinders. In our case, the slices are not parallel, and the partial bone surface is not a closed surface. Therefore, these approaches are not adapted to our problem.

For each slice i, the algorithm first computes an approximation of the bone slice center $c(i)$. Using these central points, it approximates a line corresponding to the central axis of the bone. Then, for each slice, it:

1) Updates the value of $c(i)$ as the intersection point of the line and the corresponding slice plane;
2) Casts rays from the center toward the surface at regular intervals (spaced by angle θ);
3) Computes the new vertex as the intersection between rays and segments connecting the original points (at distance r from the center).

This first parametrization of the surface provides us with a homogeneous re-sampling of the original set of points in a suitable grid form, with a mean distance of 0.14 mm between the original and the re-sampled points.

D. Surface Reconstruction using B-Splines

Let $P_{i,j}$ for $i = 1, ..., m$ and $j = 1, ... n$ be the points of the grid obtained from the previous re-parametrization. We will fit a Tensor Product B-Spline Surface $BS : (u,v) \mapsto p \in S_{bone}$ on this grid using a Least Squares approximation procedure proposed by Carl Boor in [9].

Given order p and q, and the number of control points e and f for the u and v directions respectively, finding the B-Spline surface of minimum Least Squares (LS) distance to the grid is a non-linear optimization problem. However, it may be approached using a B-Spline curve LS approximation, which is reduced to the resolution of a linear system. The procedure consists of the following steps:

- Apply curve approximation to each column of data points to compute a set of $(e + 1)$ data points, which form a grid of $(e+1) \times (n+1)$ intermediate data points.
- Apply curve approximation to each row of these intermediate data points to compute the desired control points. Since each row has $n+1$ intermediate data points and there are $e + 1$ rows, each approximation for a row generates $f + 1$ desired control points, and, as a result, we will finally obtain $(e + 1) \times (f + 1)$ control points.

The approximating B-Spline surface is obtained after solving $(n + 1) \times (e + 1)$ linear systems. m is the number of image slices (between 50 and 250 for our data) and n the number of rays for the re-sampling step, that we fixed at 15. e and f must be chosen depending on the form of the bones. For elongated bones as the ulna and radius, typical values are $e = 15$ and $f = 5$. For this work we used quadratic splines ($p = q = 2$). The computation time for this step is usually less than 1 second.

The surface approximation step ensures a smooth surface and helps to overcome the problem of segmentation false positives.
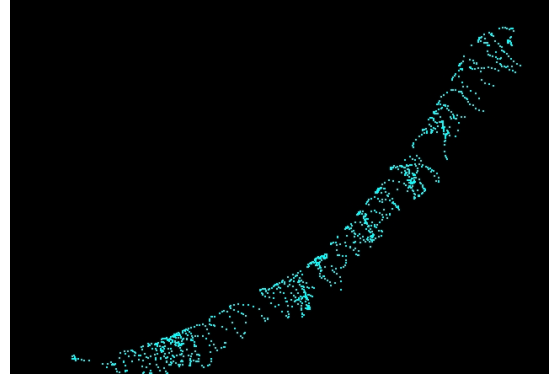

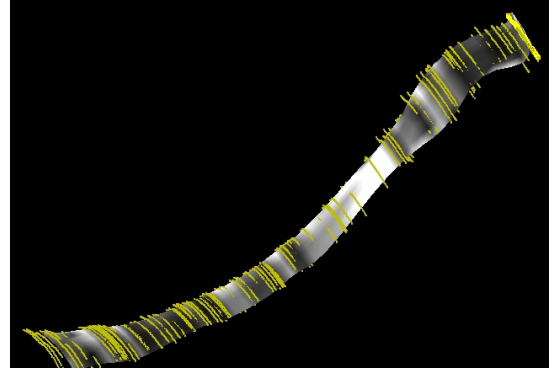Fig. 3. Points sampled from the clavicle phantom

Fig. 4. Reconstructed upper surface of a clavicle phantom model. Yellow points represent the 2D segmentation output.

III. RESULTS ON PHANTOM MODELS AND REAL BONES

In order to measure the error of our reconstruction approach, we used a phantom model (a dry bone) of a clavicle as our gold standard. We first obtained a sample of 1145 localized surface points (see Fig. 3). These points were digitized from the dry bone surface thanks to the Surgetics digitizing probe, such as in [10]. Keeping the bone in the same position, we then performed a series of US acquisitions and applied our surface reconstruction method.

The result is shown on Fig. 4. The yellow points represent the 2D segmentation output, and the gray intensity texture of the approximated B-Spline surface corresponds to the euclidean distance between the surface and the closest segmented point. The mean distance from the surface to the point cloud for several spline parameters is shown in Table I. Even though a greater number of control points leads to a smaller approximation error, it is better to choose a low number (10 to 15 gives the best results for our data) in order to keep on control the smoothness of the surface. Using as many control points as data points yields an interpolation of the original surface, where small segmentation errors cause bad surface topology and unsuitable folds (see Fig. 5 and 6). To ensure a good topology, a compromise must be found.

Also, in order to compare the extracted surface to a gold standard, the experiment has been made with phantom data where the segmentation performance is at its best and no false positives are obtained. As a result, the reconstruction
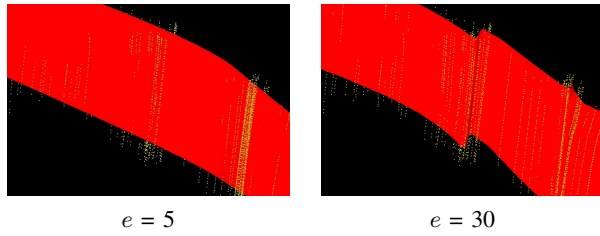
$e = 5$ $e = 30$
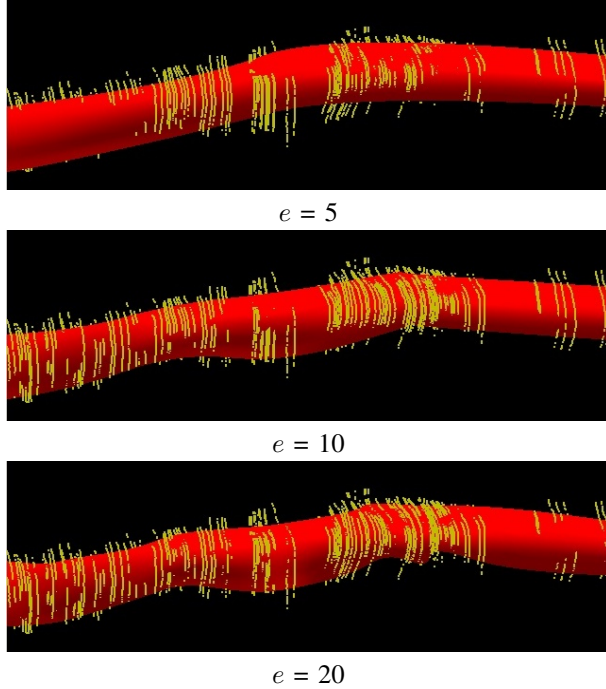
Fig. 5. Reconstructed surface of a real ulna with different values of e

$e = 5$

$e = 10$

$e = 20$

Fig. 6. Reconstructed surface of a real radius. Results for different numbers of Control Points.

Fig. 7. Reconstructed radius and ulna. Data scanned from a real subject (a vivid human being).

TABLE I

AVERAGE RECONSTRUCTION ERROR

Number of Control Points	Average distance (cm)
5	1.71
10	1.32
15	1.26
20	1.16

CAD system.

error does not reflect the utility of an approximating spline using a low number of control points to attenuate the effect of false positive segmentation results. Further validation will cover this point.

Fig. 6 and 7 show the output of our algorithm for a series of US images of a real forearm from a healthy subject. Even though we leave to future work the validation of our approach on this kind of data, the results are visually very encouraging.

IV. CONCLUSION AND PERSPECTIVES

We have presented a fully automatic method for reconstructing partial bone surfaces from a series of localized B-mode US scans. The segmentation scheme has been subject to validation in [4] for semi-automatic segmentation. The surface approximation step ensures a smooth topology and helps overcome the segmentation outliers.

We have obtained encouraging results from our approach with a physical phantom model of clavicle, obtaining an error of 1,16mm (see Sect. III). We also have presented examples on real data built from several bones.

Ongoing work focuses on validation on a extended data set, measuring intra-operator variability, and application to a

REFERENCES

[1] J. A. Noble and D. Boukerroui, "Ultrasound image segmentation: A survey," *IEEE Transactions on Medical Imaging*, vol. 25, no. 8, pp. 987–1010, 2006.
[2] Y. Yu and S. T. Acton, "Segmentation of ultrasound imagery using anisotropic diffusion," in *Asilomar Conference on signals systems and computers*, 2001, pp. 1151–1155.
[3] C. Tauber, H. Batatia, and A. Ayache, "Robust b-spline snakes for ultrasound image segmentation," in *IEEE Computers in Cardiology*, 2004.
[4] A. Alfiansyah, "Intégration de données ultrasonores per-opératoires dans le geste de chirurgie orthopédique assisté par ordinateur," Ph.D. dissertation, Université de la Méditerranée, 2007.
[5] A. Alfiansyah, R. Streinchenberger, P. Kilian, M.-E. Bellemare, and O. Coulon, "Automatic segmentation of hip bone surface in ultrasound images using an active contour," in *International Conference on Computer Assisted Radiology and Surgery (CARS '06)*, 2006.
[6] T. Ju, J. D. Warren, J. Carson, G. Eichele, C. Thaller, W. Chiu, M. Bello, and I. A. Kakadiaris, "Building 3d surface networks from 2d curve networks with application to anatomical modeling," *The Visual Computer*, pp. 764–773, 2005.
[7] R. Klein, A. Schilling, and W. Straer, "Reconstruction and simplification of surfaces from contours," *Graphical Models*, no. 6, pp. 429–443, 2000.
[8] K. Krissian, R. Kikinis, and C.-F. Westin, "Algorithms for extracting vessel centerlines," Laboratory of Mathematics in Imaging, Tech. Rep. 3, 2004.
[9] C. de Boor, *Practical Guide to Slpines*. Springer Verlag, 1994.
[10] P. Kilian, M.-E. Bellemare, and C. Plaskos, "Ultrasound acquisitions for minimally invasive knee surgery using morphometric models - An accuracy analysis," in *5th Annual Meeting of the International Society for Computer Assisted Orthopaedic Surgery (CAOS '05)*. CAOS International, 2005, pp. 240– 243.